Proceedings of the ASME 2013 Dynamic Systems and Control Conference
DSCC2013
October 21-23, 2013, Palo Alto, California, USA

DSCC2013-3894

POD-GALERKIN-REDUCED MODEL PREDICTIVE CONTROL FOR RADIATIVE DRYING OF COATINGS

Xiaoqing Cao
International Center for Automotive Research
Clemson University
Greenville, SC 29607
Xiaoqin@g.clemson.edu

Beshah Ayalew
International Center for Automotive Research
Clemson University
Greenville, SC 29607
beshah@clemson.edu

ABSTRACT
The process of drying coatings constitutes an important step in automotive plants. In this paper, a control scheme for infrared drying of waterborne coatings is outlined and demonstrated. The drying process model, which is described by a coupled system of a nonlinear partial differential equation for moisture content and a nonlinear ordinary differential equation for coating temperature, is first reduced to a system of nonlinear ODEs using the POD-Galerkin method. Then, a nonlinear model predictive control framework is devised to track a prescribed moisture removal profile during the drying process, while optimizing energy consumption and quality criteria. The effectiveness of the approach is demonstrated using system simulations.

NOMENCLATURE
$\mathcal{M}$ Moisture content (kg water/kg solid)
$\bar{\mathcal{M}}$ Average moisture content
z Distance to bottom in Euler coordinate
ξ Anhydrous distance to bottom in Lagrangian coordinate
ξ_d Thickness of the anhydrous solid.
ε Shrinkage coefficient
T Temperature
ρ Density
C Specific heat
$\mathcal{L}$ Latent heat of water vaporization
α_{abs} Absorption coefficient

I. INTRODUCTION
In automotive manufacturing, the painting process involves a set of steps designed to impart good corrosion and scratch resistance properties as well as glossy appearances that meet customer expectations. Such requirements of high coating quality are often achieved at the expense of high energy consumption and environmental pollution [1, 2].

Conventionally, organic solvents are commonly used in automotive coatings due to their property of easy evaporation. However, volatile organic compounds (VOCs) contained in these organic solvents contribute to ground-level ozone formation [2]. With stricter regulations on VOC emissions and higher cost of petroleum-based solvents, more and more automotive original equipment manufacturers (OEMs) are switching from organic solvent-based paints to waterborne paints. Since water is less volatile than some solvents, the use of waterborne paints faces critical issues such as longer flash-off time and popping phenomenon, which necessitate tight control over the drying process.

The use of an infrared radiative (IR) heat source, possibly in conjunction with the convective booth, is a potential alternative to the current process of drying waterborne paints [1, 3-5]. When the IR source's emission wavelength is properly matched with the absorption spectra of the target paint material (including water), infrared radiation can transfer energy directly to the paint material without heating the convective air and the substrate. Thus, much higher energy efficiency can be achieved compared to current convective bake-ovens. Moreover, IR is also reported to have higher power density, faster response and better controllability compared with convective bake-ovens [6].

To devise suitable process control systems for IR drying, process models are needed to understand the behavior of the drying process. The first principle models of drying consist of coupled heat and mass transfer processes represented by nonlinear parabolic partial differential equations (PDEs). Due to the strong nonlinearity of and the infinite dimensional (distributed parameter) nature of these models, analytical solutions are often out of reach, and numerical solutions are computationally intensive as well. Thus, reduced order models (ROMs) are often derived by approximating the dominant spatial and temporal dynamics. Specifically, the behavior of parabolic PDE system can be approximated by a linear combination of a finite set of basis functions [7]. Proper orthogonal decomposition (POD) is an effective way to find such an optimal set of basis functions that captures the dominant spatial dynamics of the PDE system [8-11]. These basis functions can then be incorporated in some weighted residual method, such as Galerkin projection [12], to derive reduced order models thereby changing the nonlinear PDEs to nonlinear ODEs. The control strategy could then be designed based on these reduced order models.

As far as suitable control strategies to apply, one finds that model predictive control (MPC) has been one of the most successful control strategies widely used in the modern process industry [13, 14]. In [15], a multivariable MPC is formulated and applied to regulate the moisture content and temperature of a thin fiber material in an infrared-convective dryer. However, this controller was applied to a simplified linear system model obtained by a minimum realization. Dufour et al. proposed a two-level optimization scheme for infrared-convective drying of a paint film [16-18]. The nonlinear system PDE is first linearized based on a pre-defined nominal input. Then, the linear model is used to find optimal input variations with on-line predictive control. Reference temperature/moisture trajectories were pre-designed and tracked on-line to achieve a good drying performance. Although temperature/moisture tracking can be achieved with certain accuracy under this linear MPC scheme, nonlinear MPC is a more natural choice for nonlinear PDE systems because of the limitation of the operation range of linearization methods. Moreover, since system nonlinearity is preserved in nonlinear MPC schemes, control performance can be expected to improve.

Motivated by the potential of POD-Galerkin method for nonlinear parabolic PDEs and the success of linear MPC in infrared-convective drying process [16-18], this paper proposes and demonstrates a POD-Galerkin based nonlinear MPC scheme for drying waterborne automotive coatings. The objective of the nonlinear MPC will be to track a prescribed drying profile, while optimizing energy consumption and maintaining certain surface quality criteria.

The rest of the paper is organized as follows: In Section II, the detailed model of the drying process is outlined and in Section III, the POD-Galerkin method is applied to the drying model. Section IV outlines the nonlinear MPC scheme, along with the selection of the specific objective functions for the drying process. Section V gives demonstrative simulation results, including comparisons with online-linearization based MPC (LMPC) described in [16-18]. Conclusions are provided in Section VI.

II. DRYING PROCESS MODEL

Studies on process models and the effects of parameters on paint drying have already been conducted in [19-22]. For the purposes of this paper, a schematic of the infrared-convective drying setup is shown in Fig. 1. Both mass and heat transfer are assumed to take place in the direction perpendicular to the paint surface. As a result, moisture content $\mathcal{M}$ is spatially distributed along the z direction. Moreover, as pointed out in other works [17, 23-25], the temperature difference between the top and bottom layers are negligible since the coating is usually very thin (around 20 μm for basecoat and 100 μm in total [21]). Thus, the temperature of the paint is assumed to be spatially uniform during the drying process.

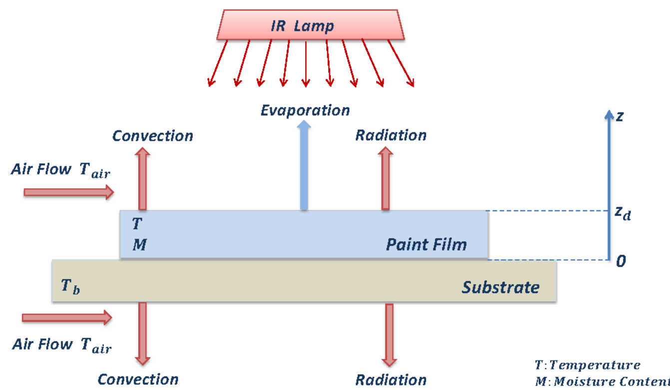

FIGURE 1. INFRARED DRYING SYSTEM

The mass transfer during drying constitutes water diffusion and evaporation. With the evaporation of water from the surface, the volume of paint material changes, leading to the shrinkage phenomenon. This shrinkage is better handled by Lagrangian coordinates (ξ, t) instead of Euler coordinates (z, t). The relationship between these two coordinates is given by [17, 26]:

$$\frac{d\xi}{dz} = \frac{1}{1 + \varepsilon\bar{\mathcal{M}}} \tag{1}$$

where ε is the shrinkage coefficient which depends on the characteristics of the paint material and $\bar{\mathcal{M}}$ is the average moisture content.

The mass transfer equation follows from Fick's law [27]:

$$\frac{\partial \mathcal{M}}{\partial t} = \frac{\partial}{\partial \xi}\left[D(\mathcal{M}, T)\frac{\partial \mathcal{M}}{\partial \xi}\right] \tag{2}$$

where $\xi \in [0, \xi_d]$ and with two boundary conditions at the top and bottom:

$$-D(\mathcal{M},T)\frac{\partial \mathcal{M}}{\partial \xi}=\frac{\dot{m}(\bar{\mathcal{M}},T)}{\rho_d}, \quad at\ \xi=\xi_d \tag{3}$$

$$\frac{\partial \mathcal{M}}{\partial \xi}=0\,, \qquad at\ \xi=0 \tag{4}$$

$D(\mathcal{M},T)$ is the nonlinear diffusion coefficient which depends on the moisture content $\mathcal{M}$ and temperature T, according to:

$$D(\mathcal{M},T)=\frac{D_0 e^{(-a/\mathcal{M})}e^{(-E/RT)}}{(1+\varepsilon\mathcal{M})^2} \tag{5}$$

$\dot{m}(\mathcal{M},T)$ is the mass transfer rate on the film surface and is driven by the vapor pressure difference between ambient air and the coating film. The expression of $\dot{m}(\mathcal{M},T)$ is given by the following equation [16]:

$$\dot{m}(\bar{\mathcal{M}},T)=\frac{k_m m_v}{R}p_t\frac{2}{T+T_{air}}log_{10}\left[\frac{p_t-\mathcal{M}_{air}\cdot p_{sat}(T_{air})}{p_t-a(\bar{\mathcal{M}})\cdot p_{sat}(T)}\right] \tag{6}$$

Detailed description of the above equations can be found in [16].

Considering energy transfer under the uniform temperature (thin coating) assumption, the energy balance equation can be written as:

$$\left(\rho_p C_p z_p+\rho_s C_s z_s\right)\frac{dT}{dt}=P_{abs}-P_l-P_{rad}-P_{conv} \tag{7}$$

where $P_{abs}=\alpha_{abs}P_{IR}$ is the heat energy absorbed by the paint material, α_{abs} is the IR absorptivity of the paint material and P_{IR} is the heat flux from IR lamp (heat source); $P_l=\mathcal{L}(T)\dot{m}(\bar{\mathcal{M}},T)$ is the latent heat dissipated with the evaporation of water; $P_{rad}=\sigma_1(T^4-T_{air}^4)+\sigma_2(T^4-T_b^4)$ and $P_{conv}=h_c(T-T_{air})+h_c(T-T_b)$ are radiative and convective heat transfer between the paint film and ambient (T_{air}) as well as the substrate and ambient (T_b). Index p and s in the left-hand side of Eq. (7) stand for paint and substrate, respectively. Reference [5] has shown experimental validation of the above drying model.

It can be seen that, due to the complex and nonlinear dependence of the diffusion coefficient D and the mass transfer rate $\dot{m}$ on the system states $(\mathcal{M},T)$, the PDE in Eq. (2) is highly nonlinear. Moreover, it is coupled with the dynamics of the temperature T given by the ODE in Eq. (7).

III. POD-GALERKIN METHOD

Proper Orthogonal Decomposition

Proper orthogonal decomposition (POD) is a powerful model reduction method of high dimensional systems [28, 29]. It is also known as principal component analysis, Karhunen–Loeve decomposition and singular value decomposition (SVD) [30]. The basic idea of this method is to generate a set of independent basis functions from simulated or experimental data. The state variable is sought to be approximated in the following form:

$$x(z,t)\cong\sum_{k=1}^{N}a_k(t)\,\varphi_k(z) \tag{8}$$

where $x(z,t)$ is the state variable of the distributed parameter system, $\varphi_k(z)$ are basis functions that represent the dominant spatial distribution modes and $a_k(t)$ are temporal amplitudes of the corresponding basis functions. $N\in\mathbb{R}$ is the selected number of the POD basis functions. With sufficiently large basis function number N, the POD approximation is expected to converge to the actual $x(z,t)$.

For convenience of practical implementation, both spatial and temporal discretizations are adopted. Consider a given set of sampled data (snapshot): $X=[x_1 \ ,\dots,\ x_m]$, $x_i\in\mathbb{R}^n(i=1,\dots,m)$, where $n\in\mathbb{R}$ is the size of spatial discretization and $m\in\mathbb{R}$ is the size of temporal discretization. The objective of POD is to obtain a reduced N dimensional subspace $V_{sub}\subset V, V\in\mathbb{R}^n$ such that the linear combination of basis vectors from this subspace can approximate the original sampled data X optimally, in the least-square sense [8]. Let $V_{sub}=span\,\{\tilde{\varphi}_1,\cdots,\tilde{\varphi}_N\}$, the problem can be transferred to one of finding orthogonal basis vectors $\tilde{\varphi}_i(i=1,\cdots,N)$, such that the following error is minimized [31, 32]:

$$Min\ \frac{1}{m}\sum_{i=1}^{m}\left\|x_i-\sum_{k=1}^{N}(x_i,\tilde{\varphi}_k)\tilde{\varphi}_k\right\|^2 \tag{9}$$

where $(\cdot,\cdot)$ denotes the standard $\mathcal{L}^2$ inner product and $\|x\|=\sqrt{x^Tx}$. The POD basis vectors satisfy orthogonality:

$$\left(\tilde{\varphi}_i,\tilde{\varphi}_j\right)=\delta_{ij} \tag{10}$$

$\delta_{ij}(i,j=1,\dots,N)$ is the commonly defined Kronecker delta function. The solution of Eq. (8) can be found by defining a correlation matrix between x_i and $x_j(i,j=1,\cdots,m)$, and deriving the POD basis vectors from the resulting eigenvalue problems [7, 8, 10]. A more practical way to extract POD basis vectors from sampled data is to use SVD [8, 10, 33]. Applying SVD to the snapshot $X\in\mathbb{R}^{n*m}$, we have:

$$X=U\Sigma V^* \tag{11}$$

where $U\in\mathbb{R}^{n*n}$, $V\in\mathbb{R}^{m*m}$ are orthogonal unitary matrices and $\Sigma=\begin{pmatrix}\Sigma_r & 0\\ 0 & 0\end{pmatrix}\in\mathbb{R}^{n*m}$, $\Sigma_r=diag(\sigma_1,\dots,\sigma_r)$. σ_i are the singular values of matrix X and are arranged in the order: $\sigma_1\geq\sigma_2\geq\cdots\geq\sigma_r$. Then, the first r columns of U are the orthogonal POD basis vectors $(\tilde{\varphi}_1,\cdots,\tilde{\varphi}_r)$. The POD basis functions $\varphi_k(z)$ $(k=1,\dots,r)$ can be obtained by interpolation from the corresponding $\widetilde{\varphi}_k$. Then, the spatial distribution of the state variables can be approximated by the first γ POD basis functions $x(z,t) \cong \sum_{k=1}^{\gamma} a_k(t)\varphi_k(z)$ with an approximation accuracy given by:

$$A(\gamma) = \frac{\sum_{i=1}^{\gamma} \sigma_i}{\sum_{j=1}^{r} \sigma_j} \tag{12}$$

For a given POD order, the approximation accuracy can be determined from Eq. (12).

Once the spatial variation is approximated, the Galerkin projection method can be applied to obtain the dynamics of temporal coefficients $a_k(t)$. This is briefly reviewed next.

Galerkin Method

The Galerkin projection is a kind of weighted residual method which can be used to determine the temporal coefficient $a_k(t)$ via a pseudo-modal analysis [12]. Suppose the dynamic equation for a general nonlinear distributed parameter system is expressed as:

$$\frac{\partial x(z,t)}{\partial t} = Ax(z,t) + f(z,t) \tag{13}$$

where A is a nonlinear spatial differential operator and $f(z,t)$ is a general nonlinear function. Suppose the solution of Eq. (13) can be represented by a set of basis functions $\psi_l(z)(l = 1, \ldots, L)$:

$$x(z,t) \cong \sum_{l=1}^{L} a_l(t)\,\psi_l(z) = \hat{x}(z,t) \tag{14}$$

Once the basis functions are derived, coefficients $a_l(t)$ can be determined by the method of weighted residuals. The idea is to determine $a_l(t)$ such that the residual:

$$R_e(z,t) = \frac{\partial \hat{x}(z,t)}{\partial t} - A\hat{x}(z,t) - f(z,t) \tag{15}$$

is small under the criterion that the weighted residual vanishes:

$$\int \omega_l \cdot R_e(z,t)dz = 0 \quad (\, l = 1, \cdots, L) \tag{16}$$

Different choices of the weighting functions ω_l lead to different weighted residual methods. In the Galerkin method, the weighting functions are selected to be the basis functions themselves. That is:

$$\int \psi_l(z) \cdot R_e(z,t)dz = 0 \quad (\, l = 1, \cdots, L) \tag{17}$$

POD-Galerkin Methods for the Drying Model

We now apply the POD-Galerkin method to the drying model described in Section II. Assume that an initial set of process snapshots are available, either from experiment or from simulation. Using SVD, a set of POD basis functions $\varphi_l(l = 1, \cdots, L)$ can be calculated. With the POD approximation:

$$\widehat{\mathcal{M}}(\xi,t) = \sum_{l=1}^{L} a_l(t)\,\varphi_l(\xi) \tag{18}$$

the residual for the PDE model in Eq. (2) can be written as:

$$R_e(\xi,t) = \frac{\partial \widehat{\mathcal{M}}}{\partial t} - \frac{\partial}{\partial \xi}\left[D\big(\widehat{\mathcal{M}},T\big)\frac{\partial \widehat{\mathcal{M}}}{\partial \xi}\right] \tag{19}$$

After applying the Galerkin method, we can obtain:

$$\left(\varphi_j, \frac{\partial \sum_{l=1}^{L} a_l\,\varphi_l}{\partial t}\right) = \left(\varphi_j, \frac{\partial}{\partial \xi}\left[D\left(\sum_{l=1}^{L} a_l\,\varphi_l, T\right)\frac{\partial \sum_{l=1}^{L} a_l\,\varphi_l}{\partial \xi}\right]\right) \tag{20}$$

With the orthogonal property and boundary conditions given in Eqs. (3) and (4), the above equation can be reduced to:

$$\dot{a}_j(t) = -\int_0^{\xi_d} D\left(\sum_{l=1}^{L} a_l\,\varphi_l, T\right) \cdot \frac{\partial \sum_{l=1}^{L} a_l\,\varphi_l}{\partial \xi} \cdot \frac{d\varphi_j}{d\xi}\,d\xi + \left(\varphi_j \cdot \frac{-\dot{m}(\overline{\mathcal{M}},T)}{\rho_d}\right)\Big|_{\xi_d} \tag{21}$$

where $j = 1, \cdots, L$.

The initial value of temporal coefficients can be obtained from: $a_{k0} = \int x(z,0)\varphi_k(z)dz$ [31].

The above nonlinear ODE in Eq. (21) describes the evolution of the j^{th} temporal coefficient corresponding to the j^{th} POD basis function. The solutions of Eq. (21) combined with POD basis functions give an approximate numerical solution for the PDE in Eq. (2).

The approximation accuracy of POD-Galerkin method can be adjusted by choosing the number of POD basis functions according to Eq. (12). It may not be realistic to assume that the POD basis functions from initial snapshots can capture all the dominant spatial modes of nonlinear dynamic system. A possible solution is to update the POD basis functions with new snapshots as they become available (online update).

IV. NONLINEAR MODEL PREDICTIVE CONTROL

The main idea of MPC is to use an explicit plant model to predict system behaviors in a prediction horizon. Within the prediction horizon, an optimal open-loop input sequence is generated to satisfy desired optimization criteria and the constraints of the process. Only the first input in this optimal sequence is often applied to the actual plant. Then, new measurements and model updates are conducted, the process is repeated using a receding prediction horizon.

In this paper, a nonlinear MPC scheme (NMPC) shown in Fig. 2 is proposed for the drying process. This POD-NMPC scheme is implemented under the assumptions that an acceptable and computationally tractable reduced model is available and snapshots can be obtained from the plant (or its original model for the simulation-based analysis we pursue here). From some initial snapshots from the plant, the POD basis functions are calculated and the original PDE is reduced to nonlinear ODEs in terms of the temporal coefficients. A constrained optimization is run for the prediction horizon to generate an optimal input sequence that minimizes the objective/cost function. The first input of the optimal sequence is applied to the plant and when new snapshots are available, the next iteration of POD-NMPC scheme begins.

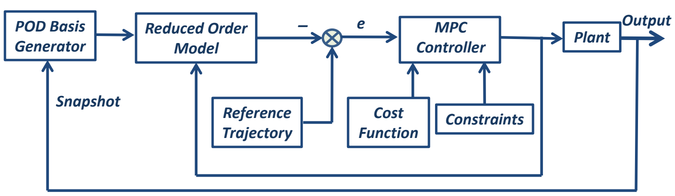

FIGURE 2. POD-NMPC SCHEME

The remaining issue in formulating model predictive control for the drying problem is to define proper objective functions such that the control input (infrared power) is optimized for different criteria such as moisture content, paint quality, energy consumption, etc. Three possible choices are discussed below.

In the application of paint drying, the first objective is to get the paint material dried according to a specified drying profile such that subsequent processes like curing can proceed without causing defects. This objective can be posed as tracking a desired average moisture distribution $\bar{\mathcal{M}}_{ref}(t)$ during the drying process. The discretized objective function under the MPC framework can be defined as:

$$J_A(k) = \sum_{i=1}^{H_p} \alpha_i\left(\bar{\mathcal{M}}(k+i) - \bar{\mathcal{M}}_{ref}(k+i)\right)^2 \quad (22)$$

where H_p is the length of prediction horizon, k is the current time instant. α_i are the weighted coefficients assigned to tracking errors within the horizon and $\bar{\mathcal{M}}(k+i)$ stands for the average moisture content in i^{th} prediction horizon.

In addition to moisture content, quality property is another important drying objective, which has to be achieved in order to have a good corrosion and scratch protection performance as well as lustrous appearances of the final product. Several quality criteria could be considered. One may consider the most natural criterion to be uniform drying, which means no spatial moisture gradient exists during the drying process. However, this quality objective is not realistic with the current drying setup since the moisture concentration is spatially distributed the instant evaporation at the top commences and no compensation can be made at the bottom where no evaporation happens. Another possible quality index is maximum surface gradient with time. Allanic *et al.* pointed out in [23] that the surface deterioration is due to early surface drying in the first drying stage, which has to be mitigated if possible. They suggested the objective function to penalize the surface moisture gradient in time:

$$J_B(k) = \max_i \left\{\beta_i\left(\dot{\mathcal{M}}_s(k+i)\right)^2\right\} \quad (23)$$

$i = 1, \ldots, H_p$. $\mathcal{M}_s$ stands for the surface moisture content and β_i are weighted coefficients.

Energy consumption should also be considered as a control objective since the paint drying process is energy intensive and is reported to contribute most to the total energy used in automotive manufacturing [3]. A suitable form to penalize energy consumption is:

$$J_C(k) = \sum_{i=1}^{H_p} \gamma_i\left(P_{IR}(k+i)\right)^2 \quad (24)$$

The final form of the constrained optimization problem for NMPC of infrared drying can then be written as:

$$\min_{U(k)} J(k) \quad (25)$$

where $J(k) = J_A(k) + J_B(k) + J_C(k)$ with
$U(k) = \left[P_{IR}(k), P_{IR}(k+1), \ldots, P_{IR}(k+H_p-1)\right]^T$

Subject to the constraints:

$$\left(\rho_p C_p z_p + \rho_s C_s z_s\right)\frac{dT(k+i)}{dt} = P_{abs}(k+i) - P_l(k+i) - P_{rad}(k+i) - P_{conv}(k+i)$$

$$\dot{a}_j(k+i) = \left(\varphi_j \cdot \frac{-\dot{m}(\bar{\mathcal{M}},T)}{\rho_d}\right)\Big|_{\xi_d} - \int_0^{\xi_d} D\left(\textstyle\sum_{l=1}^{L} a_l\varphi_l, T\right)\cdot \frac{\partial \sum_{l=1}^{L} a_l\varphi_l}{\partial \xi}\cdot\frac{d\varphi_j}{d\xi}\, d\xi$$

$$0 \le P_{IR}(k+i) \le P_{max}, \; -\Delta P_{max} \le \nabla P_{IR}(k+i) \le \Delta P_{max}$$

$$i = 1, \cdots, H_p; \quad j = 1, \cdots, L.$$

The last two inequalities are input constraints on the total power available and the rate of power change. They are subject to the physical properties of the IR heat source used in the plant setup. By solving the above optimization problem, an optimal input sequence $U(k)$ is obtained. The first input in the sequence can be applied as the control input at time instant k, and the process is repeated.

V. RESULTS AND DISCUSSIONS

To verify the proposed POD-NMPC method for the control of drying processes, simulations were conducted based on the drying model in Eq. (2) and Eq. (7). Detailed parameters in the drying model can be found in [16]. The main control objective of this simulation is to track a pre-defined average moisture profile, which characterizes the typical desired drying profile of the paint material applied. Other simulation conditions are listed as follows:

Simulation time: t=150 s; Sample time t_s=0.1 s;
Snapshot time=1 s; Number of POD basis=2;
NMPC prediction horizon: $H_p = 5$;
Control input constraints: $P_{max} = 9000\ W/m^2$;
$\Delta P_{max} = 1000\ W/m^2$;
Initial condition: $\mathcal{M}_{ini} = 0.3\ kg/kg$, $T_b = 293\ K$, $T_{air} = 325\ K$.

With 2 POD basis functions, the minimum accuracy of POD approximation is 99.996%, according to Eq. (12).

Fig. 3 — Fig. 6 show the simulation results with the proposed control scheme. A comparison was made between the NMPC cases with only drying profile consideration (J_A) and with quality/energy considerations (total J). Fig. 3 shows top/bottom moisture content during drying. Asymmetric evaporation (only from the top surface) and diffusion within the paint lead to the unevenly distributed moisture content. Moreover, with the painting quality criterion Eq. (23) in the objective function, the surface drying rate is slower than that without quality consideration at the beginning of drying. This helps to address the early surface drying issue [23]. The tracking error of average moisture is shown in Fig. 4. With only moisture tracking in the objective, the tracking error stays relatively small over the process. However, when additional considerations of quality and energy are added, the moisture tracking performance of the proposed controller degrades as a tradeoff. Fig. 5 shows the comparison of control inputs. It is clear that at the beginning, with the quality objective, control input is lowered to prevent large surface drying rate and at the end of drying, the heat input is also lowered to minimize the energy consumption. The total energy usage is illustrated in Fig. 6. With the inclusion of the energy criterion in the objective function, the total energy consumption is reduced as expected. This set of simulations demonstrates that the proposed POD-Galerkin based nonlinear MPC scheme is able to control the infrared drying process with selected optimization objectives. A tradeoff exists between good moisture tracking performance and improvements on quality and energy usage.

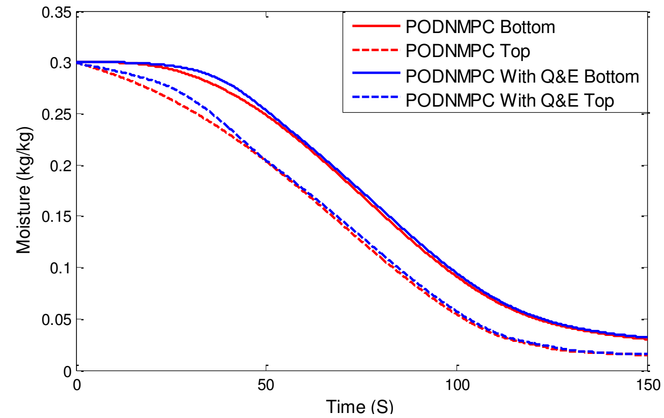

FIGURE 3. TOP-BOTTOM MOISTURE

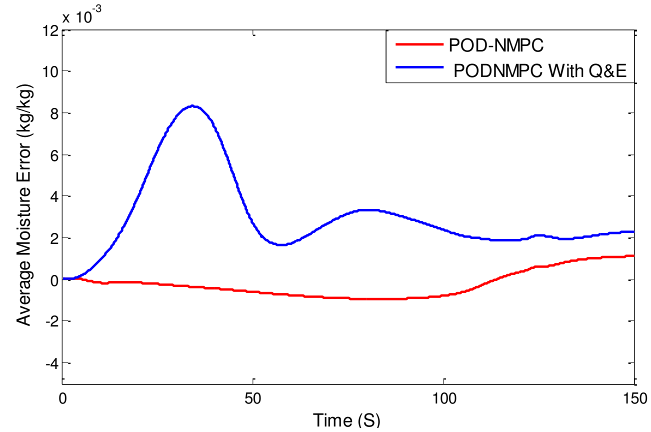

FIGURE 4. AVERAGE MOISTURE TRACKING ERROR

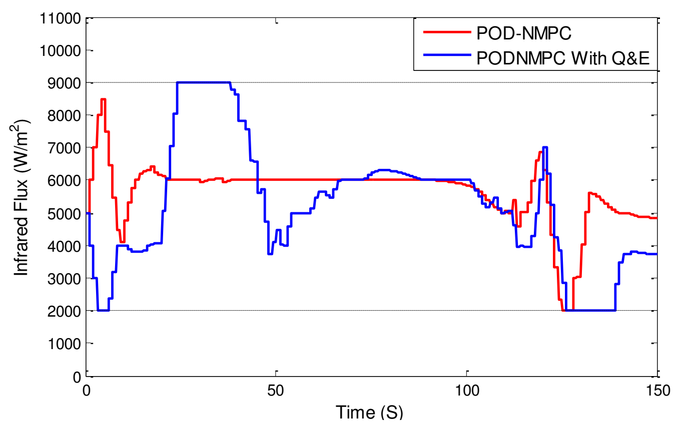

FIGURE 5. CONTROL INPUT

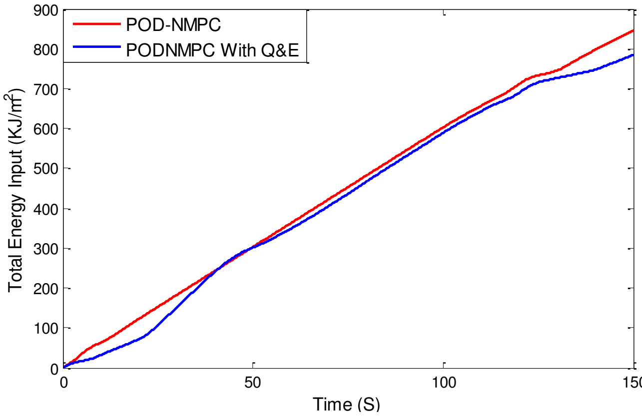

FIGURE 6. TOTAL ENERGY CONSUMPTION

To further validate the POD-NMPC method on the possible improvement of the tracking accuracy, a comparison was made between POD-NMPC and that with online-linearization based MPC (LMPC) described in [16-18]. The general idea of online linearization and offline optimization based MPC scheme is to linearize the nonlinear system PDE at offline optimized nominal points and then to apply a MPC controller to the linearized system. This control strategy is intended to deal with the nonlinearity existing in drying models and to further reduce online computational expense. However, the control accuracy of this method strongly depends on the nominal points at which the PDE is linearized. Offline optimization has to be carefully conducted before applying linear MPC control. Moreover, the linearization method itself could affect the accuracy of the system model.

The comparison of the two control schemes was conducted based on the same system model and objective function, which penalizes the average moisture tracking error (objective (J_A) for both). Initial conditions are listed above.

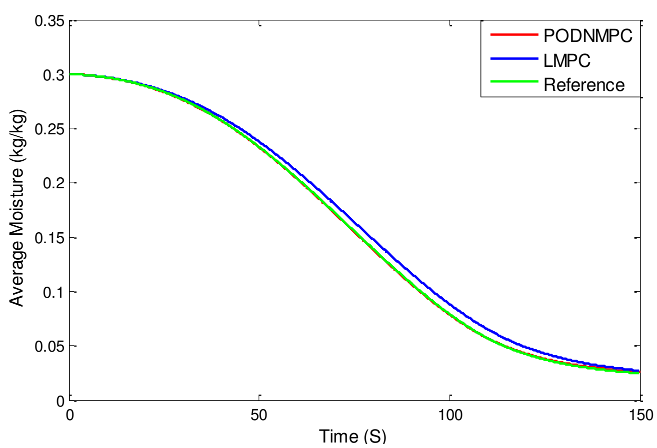

FIGURE 7. AVERAGE MOISTURE TRACKING

Figure 7 shows the comparison of the moisture tracking performance. As we can see, the average moisture profile under the linear MPC (LMPC) scheme shows a continuous deviation from the desired profile while the average moisture under the proposed control scheme is almost identical to the reference. A zoomed-in view of the differences in tracking errors between these two control schemes is demonstrated in Fig. 8. The maximum tracking error under proposed control is about $1.1 * 10^{-3}\ kg/kg$, while the linearized MPC shows an error that is almost an order of magnitude higher. The control inputs of under the two methods are shown in Fig. 9. The proposed controller adjusts the input over a wider range, especially near the beginning and the end, to achieve the tracking objective.

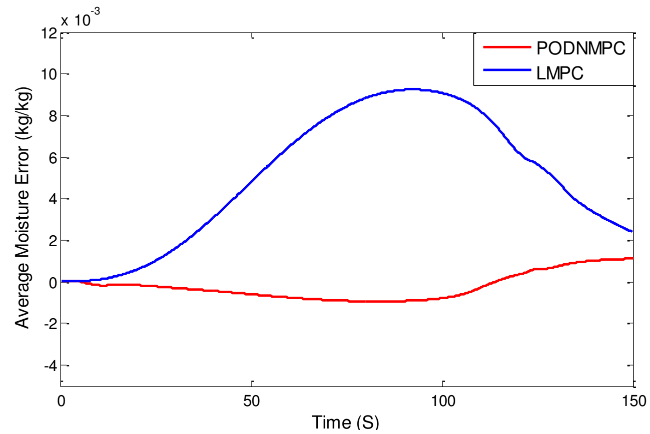

FIGURE 8. TRACKING ERRORS

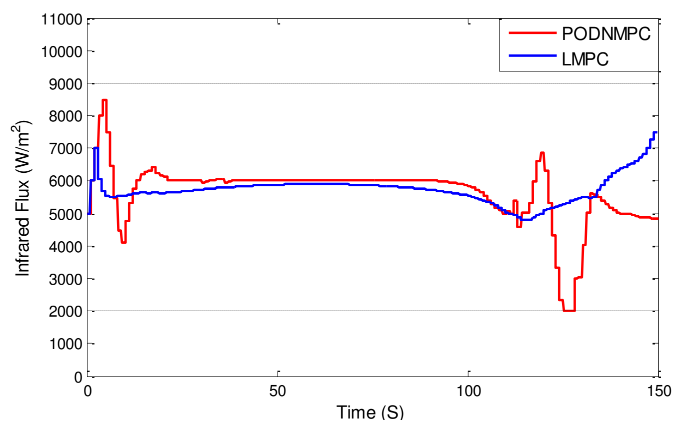

FIGURE 9. CONTROL INPUTS

VI. CONCLUSION

This paper proposed and demonstrated a POD-Galerkin based nonlinear model predictive control scheme for the control of infrared drying of waterborne coatings. The basic idea of the method is to obtain an optimal set of basis functions from available plant data using proper orthogonal decomposition, and use these basis functions to describe the dominant behavior in the spatial domain. Then, Galerkin projection method was applied with these basis functions to derive a reduced order model (set of nonlinear ODEs) from the original PDE. Based on the reduced order model, nonlinear MPC scheme was implemented that optimized criteria for moisture tracking, surface quality and energy consumption. Simulation results showed the tracking performance and the tradeoffs against energy and quality criteria under the proposed control scheme. Comparisons were included against a linearization-based MPC scheme that validated the expected improvement on moisture control accuracy (moisture tracking performance) with the proposed nonlinear MPC approach.

Some aspects need further investigations. First, the existence of optimal solution in the nonlinear MPC scheme and subsequent closed-loop stability need to be established more thoroughly, even though no difficulties were encountered in our simulation-based investigations. Second, the assumption that initial snapshot moisture profile data (and subsequent ones for that matter) are available for generating the POD basis may not be practical given sensing limitations. These issues are to be addressed in continuing studies.

ACKNOWLEDGEMENTS

This research has been supported by the National Science Foundation under the CAREER Grant no. CMMI-1055254.

REFERENCES

[1] Galitsky, C., 2008. "Energy Efficiency Improvement and Cost Saving Opportunities for the Vehicle Assembly Industry: An ENERGY STAR Guide for Energy and Plant Managers".

[2] Prendi, L., Henshaw, P., and Tam, E. K. L., 2006. "Automotive coatings with improved environmental performance". *International Journal of Environmental Studies*, 63(4), pp. 463-471.

[3] Omar, M. A., 2011. "The automotive body manufacturing systems and processes". John Wiley & Sons Ltd,, Chichester, U.K.

[4] Niemann, J., 1992. "Waterborne coatings for the automotive industry". *Progress in organic coatings*, 21(2-3), pp. 189-203.

[5] Blanc, D., Vessot, S., Laurent, P., Gerard, J., and Andrieu, J., 1997. "Study and modelling of coated car painting film by infrared or convective drying". *Drying technology*, 15(9), pp. 2303-2323.

[6] E Source Companies, L., 2005. "Curing and Drying Operations: The Pros and Cons of Infrared Heating".

[7] Shidfar, A., and Mohammadi, M., 2007. "Using empirical Eigenfunctions and Galerkin method to two - phase transport models". *Numerical Methods for Partial Differential Equations*, 23(2), pp. 456-474.

[8] Pinnau, R., 2008. "Model reduction via proper orthogonal decomposition". Model Order Reduction: Theory, Research Aspects and Applications, pp. 95-109.

[9] Luchtenburg, D., Noack, B., and Schlegel, M., 2009. "An introduction to the POD Galerkin method for fluid flows with analytical examples and MATLAB source codes". Technical Report 01/2009, Berlin Institute of Technology, Berlin, Germany.

[10] Kunisch, K., and Volkwein, S., 2001. "Galerkin proper orthogonal decomposition methods for parabolic problems". *Numerische Mathematik*, 90(1), pp. 117-148.

[11] Kunisch, K., and Volkwein, S., 2002. "Galerkin proper orthogonal decomposition methods for a general equation in fluid dynamics". *SIAM Journal on Numerical analysis*, 40(2), pp. 492-515.

[12] Ray, W. H., 1981. Advanced process control, McGraw-Hill New York.

[13] Fernandez-Camacho, E., and Bordons-Alba, C., 1995. Model predictive control in the process industry, Springer.

[14] Dufour, P., Laurent, P., and Xu, C. Z., 2004. "Model predictive control of the water based painting drying using a humidity profile soft Sensor and a temperature measurement". *Proc. Proceedings of the 14th International Drying Symposium (IDS)* .

[15] Abukhalifeh, H., Dhib, R., and Fayed, M., 2005. "Model predictive control of an infrared-convective dryer". *Drying technology*, 23(3), pp. 497-511.

[16] Larabi, M. C., Dufour, P., Laurent, P., and Touré, Y., 2000. "Predictive control of a nonlinear distributed parameter system: real time control of a painting film drying process". *Proceedings of the 14th Mathematical Theory on Network and Systems (MTNS).*

[17] Dufour, A. P. P., Blanc, D., Touré, Y., and Laurent, P., 2004. "Infrared drying process of an experimental water painting: Model predictive control". *Drying Technology*, 22(1-2), pp. 269-284.

[18] Dufour, P., Touré, Y., Blanc, D., and Laurent, P., 2003. "On nonlinear distributed parameter model predictive control strategy: on-line calculation time reduction and application to an experimental drying process". *Computers & chemical engineering*, 27(11), pp. 1533-1542.

[19] Henshaw, P., Prendi, L., and Mancina, T., 2006. "A model for the dehydration of waterborne basecoat". *Journal of Coatings Technology Research*, 3(4), pp. 285-294.

[20] Geipel, C., and Stephan, P., 2005. "Experimental investigation of the drying process of automotive base paints". *Applied Thermal Engineering*, 25(16), pp. 2578-2590.

[21] Domnick, J., Gruseck, D., Pulli, K., Scheibe, A., Ye, Q., and Brinckmann, F., 2011. "Investigations of the drying process of a water based paint film for automotive applications". *Chemical Engineering and Processing: Process Intensification*, 50(5-6), pp. 495-502.

[22] Brinckmann, F., and Stephan, P., 2011. "Experimental investigation of the drying process of water-based paints used

in automotive industry". *Chemical Engineering and Processing: Process Intensification*, 50(5-6), pp. 489-494.

[23] Allanic, N., Salagnac, P., and Glouannec, P., 2009. "Optimal constrained control of an infrared-convective drying of a polymer aqueous solution". *Chemical Engineering Research and Design*, 87(7), pp. 908-914.

[24] Allanic, N., Salagnac, P., Glouannec, P., and Guerrier, B., 2009. "Estimation of an effective water diffusion coefficient during infrared - convective drying of a polymer solution". *AIChE Journal*, 55(9), pp. 2345-2355.

[25] Brinckmann, F., Lehnhäuser, T., Löffler, R., and Stephan, P., "Simulation of the heat and mass transfer during paint drying processes". Proc. ANSYS Conference & 27th CADFEM Users' Meeting, pp. 18-20.

[26] Ruiz-Cabrera, M., Foucat, L., Bonny, J., Renou, J., and Daudin, J., 2005. "Assessment of water diffusivity in gelatine gel from moisture profiles. II. Data processing adapted to material shrinkage". *Journal of food engineering*, 68(2), pp. 221-231.

[27] Crank, J., 1979. "The mathematics of diffusion."

[28] Lumley, J., 1967. "The structure of inhomogeneous turbulent flows". Atmospheric turbulence and radio wave propagation, pp. 166-178.

[29] Sirovich, L., 1987. "Turbulence and the dynamics of coherent structures. I-Coherent structures. II-Symmetries and transformations. III-Dynamics and scaling". Quarterly of applied mathematics, 45, pp. 561-571.

[30] Wu, C., Liang, Y., Lin, W., Lee, H., and Lim, S., 2003. "A note on equivalence of proper orthogonal decomposition methods". *Journal of Sound Vibration*, 265, pp. 1103-1110.

[31] Xu, C., Ou, Y., and Schuster, E., 2011. "Sequential linear quadratic control of bilinear parabolic PDEs based on POD model reduction". *Automatica*, 47(2), pp. 418-426.

[32] Xu, C., Ou, Y., and Schuster, E., 2007. "POD-based reduced order optimal control of parabolic pde systems via diffusivity-interior-boundary actuation". *Proc. Decision and Control, 46th IEEE Conference on, IEEE*, pp. 3519-3524.

[33] Kunisch, K., and Volkwein, S., 1999. "Control of the Burgers equation by a reduced-order approach using proper orthogonal decomposition". *Journal of Optimization Theory and Applications*, 102(2), pp. 345-371.